JACS
JOURNAL OF THE AMERICAN CHEMICAL SOCIETY

Subscriber access provided by American Chemical Society

Article

Hydration Energies in the Gas Phase of Select (MX)M Ions, Where M = Na, K, Rb, Cs, NH and X = F, Cl, Br, I, NO, NO. Observed Magic Numbers of (MX)M Ions and Their Possible Significance

Arthur T. Blades, Michael Peschke, Udo H. Verkerk, and Paul Kebarle

J. Am. Chem. Soc., **2004**, 126 (38), 11995-12003• DOI: 10.1021/ja030663r • Publication Date (Web): 02 September 2004

Downloaded from http://pubs.acs.org on April 1, 2009

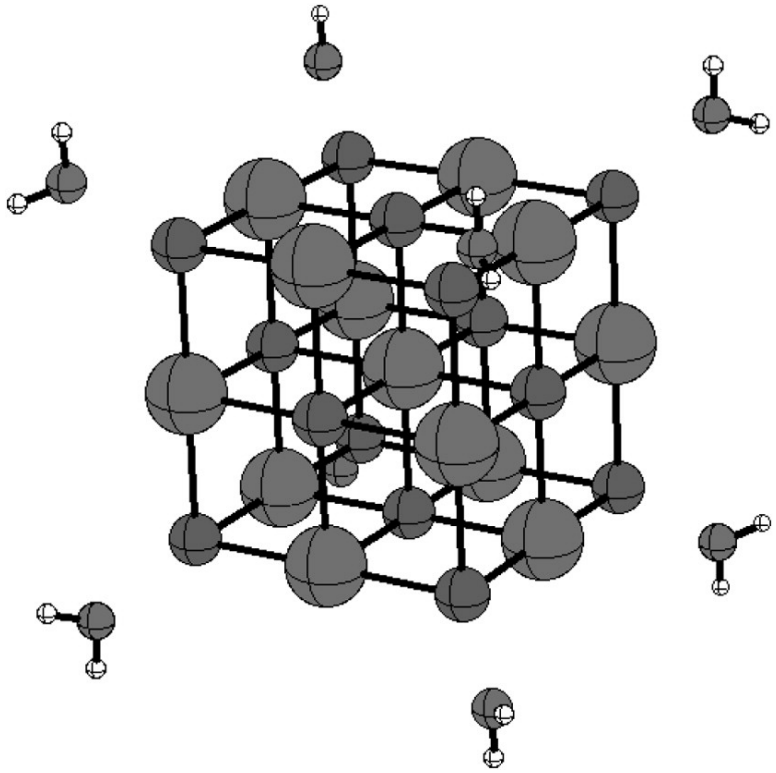

More About This Article

Additional resources and features associated with this article are available within the HTML version:

- Supporting Information
- Links to the 1 articles that cite this article, as of the time of this article download
- Access to high resolution figures
- Links to articles and content related to this article

ACS Publications
High quality. High impact.

Journal of the American Chemical Society is published by the American Chemical Society. 1155 Sixteenth Street N.W., Washington, DC 20036

JACS
JOURNAL OF THE AMERICAN CHEMICAL SOCIETY

Subscriber access provided by American Chemical Society

- Copyright permission to reproduce figures and/or text from this article

View the Full Text HTML

ACS Publications
High quality. High impact.

Journal of the American Chemical Society is published by the American Chemical Society. 1155 Sixteenth Street N.W., Washington, DC 20036

J|A|C|S
ARTICLES
Published on Web 09/02/2004

Hydration Energies in the Gas Phase of Select $(MX)_mM^+$ Ions, Where $M^+ = Na^+, K^+, Rb^+, Cs^+, NH_4^+$ and $X^- = F^-, Cl^-, Br^-, I^-, NO_2^-, NO_3^-$. Observed Magic Numbers of $(MX)_mM^+$ Ions and Their Possible Significance

Arthur T. Blades, Michael Peschke, Udo H. Verkerk, and Paul Kebarle*

Contribution from the Department of Chemistry, University of Alberta, Edmonton, Alberta, Canada T6G 2G2

Received December 15, 2003; E-mail: paul.kebarle@ualberta.ca

Abstract: The sequential hydration energies and entropies with up to four water molecules were obtained for $MXM^+ = NaFNa^+$, $NaClNa^+$, $NaBrNa^+$, $NaINa^+$, $NaNO_2Na^+$, $NaNO_3Na^+$, KFK^+, $KBrK^+$, KIK^+, $RbIRb^+$, $CsICs^+$, $NH_4BrNH_4^+$, and $NH_4INH_4^+$ from the hydration equilibria in the gas phase with a reaction chamber attached to a mass spectrometer. The MXM^+ ions as well as $(MX)_mM^+$ and higher charged ions such as $(MX)_mM_2^{2+}$ were obtained with electrospray. The observed trends of the hydration energies of MXM^+ with changing positive ion M^+ or the negative ion X^- could be rationalized on the basis of simple electrostatics. The most important contribution to the $(MXM-OH_2)^+$ bond is the interaction of the permanent and induced dipole of water with the positive charge of the nearest-neighbor M^+ ion. The repulsion due to the water dipole and the more distant X^- has a much smaller effect. Therefore, the bonding in $(MXM-OH_2)^+$ for constant M and different X ions changes very little. Similarly, for constant X and different M, the bonding follows the hydration energy trends observed for the naked M^+ ions. The sequential hydration bond energies for $MXM(H_2O)_n^+$ decrease with n in pairs, where for $n = 1$ and $n = 2$ the values are almost equal, followed by a drop in the values for $n = 3$ and $n = 4$, that again are almost equal. The hydration energies of $(MX)_mM^+$ decrease with m. The mass spectra with NaCl, obtained with electrospray and observed in the absence of water vapor, show peaks of unusually high intensities (magic numbers) at $m = 4$, 13, and 22. Experiments with variable electrical potentials in the mass spectrometer interface showed that some but not all of the ion intensity differentiation leading to magic numbers is due to collision-induced decomposition of higher mass $M(MX)_m^+$ and $M_2(MX)_m^{2+}$ ions in the interface. However, considerable magic character is retained in the absence of excitation. This result indicates that the magic ions are present also in the saturated solution of the droplets produced by electrospray and are thus representative of particularly stable nanocrystals in the saturated solution. Hydration equilibrium determinations in the gas phase demonstrated weaker hydration of the magic ion $(NaCl)_4Na^+$.

Introduction

The singly charged ion clusters $(MX)_mM^+$ as well as the multiply charged clusters, such as $(MX)_mM_2^{2+}$, of the alkali halides and other singly charged M^+, X^- ions such as NH_4^+ and NO_3^- can be of interest because they represent the initial stages of crystal nucleation and growth. They might also be useful for the understanding of surfaces and amorphous structures. When present in a solvent like water, they could be viewed also as the last stages of the dissolution of a crystal or the initial stages of crystal growth in the solution. Calculations of the binding energies of such charged and neutral clusters in the gas phase, based on electrostatic equations for the binding between the ions, began to appear in the literature in the 1970s.[1] Predictions of the relative stability of some of the structures were made.[1] At about the same time, a number of experimental observations of the clusters in the gas phase were also reported. The early work[2] was based on mass spectrometric observations of the charged clusters produced by bombardment of solid alkali halide targets by high-velocity primary ions (secondary ion mass spectrometry, SIMS). The SIMS work showed that the ion intensity distribution of a given series, such as the $(CsI)_mCs^+$ secondary ion clusters, could be smooth[2a] or exhibit some ions with higher intensities, magic number ions, expected to be of higher stability.[2b] For the $(CsI)_mCs^+$ series, typical magic numbers were found at $m = 4$, 13, and 22. These correspond to columns and rows of ions of alternating charge: $3 \times 3 \times 1$, $3 \times 3 \times 3$, and $3 \times 3 \times 5$. Standing and co-workers[2c] demonstrated that, with SIMS, the originally emitted ion distribution is smooth. However, some of these ions have sufficient internal energy to dissociate, and the dissociation generates the magic ion distribution. Subsequent experimental

(1) (a) Martin, T. P. *J. Chem. Phys.* **1978**, *69*, 2036−2042. Martin, T. P. *J. Chem. Phys.* **1980**, *72*, 3506−3510.

(2) (a) Honda, F.; Lancaster, G. M.; Fukuda, Y.; Rabalais, J. W. *J. Chem. Phys.* **1978**, *69*, 4931−4937. (b) Campana, J. E.; Barlak, T. M.; Colton, R. J.; DeCorpo, J. J.; Wyatt, J. R.; Dunlap, B. I. *Phys. Rev. Lett.* **1981**, *47*, 1046−1049. (c) Ens, W.; Beavis, R.; Standing, K. G. *Phys. Rev. Lett.* **1983**, *50*, 27−30.

work largely shifted to preparation of the cluster ions by molecular beam methods, where a rod of solid MX salt is exposed to laser flash evaporation and the evaporated material is quenched with a bath gas and further cooled by adiabatic expansion into a vacuum (vide infra).

Studies of the sequential hydration of the ion clusters in the gas phase can provide additional information. The hydration reactions could also provide an indication as to which structures are more stable. Thus, low hydration exothermicity might be associated with more stable structures. Extensive hydration will lead also to formation of lower *m* ions. Such hydration will be particularly noticeable when multiply charged $(MX)_mM_2^{2+}$ ions are present because charge separation reactions will occur that correspond to the dissolution of the cluster. Thus, the conversion of hydrated $(MX)_mM^+$ and $(MX)_mM_z^{z+}$ into hydrated M^+ and MX in the gas phase would have some semblance of the final steps in the dissolution of MX (solid) in water.

The energy changes on sequential hydration of the separated ions M^+ and X^-, determined by ion−molecule reaction equilibria and other experimental methods (positive ions,[3] negative ions[4]) and theoretical calculations (positive ions,[5] negative ions[6]), have been available for some time. The first determinations of sequential energies of hydration for the ions $(NaI)_mNa^+$ and particularly $NaINa^+$ were reported very recently by Zhang et al.,[7] who used the ion-equilibrium method to determine the hydration thermochemistry. The measurements were performed in a drift tube mass spectrometer. The $(NaI)_mNa^+$ were produced by pulsed laser vaporization of a NaI rod in He buffer gas. The plasma was cooled by a pulse of high-pressure He gas that induces cluster condensation. The resulting ions were injected, after separation by mass, into an ion drift tube containing He buffer gas and known partial pressures of H_2O. The hydration equilibria establish as the ions drift through the tube, and the relative intensities of the ions are determined with a second quadrupole mass spectrometer.[7]

In the present work, the $(MX)_mM^+$ ions are produced by electrospray ionization (ESI), a method that allows the facile generation of a great variety of ions in the gas phase,[8] including also most metal ions such as the alkali ions, group II doubly charged ions, as well as the singly and multiply charged transition metal ions.[9] On spraying salts, MX, in solvents like water, methanol, or acetonitrile at concentrations less than 10^{-5} mol/L, one observes the singly charged ion, M^+, as essentially the only species. At concentrations of 10^{-3} M or higher, one can readily observe also the ions $(MX)_mM^+$, as well as multiply charged ions $(MX)_mM_z^{z+}$, with intensities decreasing for higher *m* and *z* values. M^+ remains the major species, but the cluster ions become more and more prominent with increasing concentration. The first electrospray ionization mass spectrometry (ESIMS) study reporting such clusters seems to be the work of R. K. Boyd and co-workers[10a] (with CsI), who used the high-mass clusters for calibration of the mass to charge (*m*/*z*) scale at very high *m*/*z* values in analytical applications of ESIMS. More relevant is the recent work by M. M. Kappes and co-workers,[10b] who used ESIMS to produce alkali halide cluster ions and examined the stability of the observed ion clusters. The present work is the first use of ESIMS for studies of the hydration of the salt ion clusters.

The recent studies of the photodissociation dynamics of NaI−water clusters[11] represent related work. A variety of dissolution reactions could be observed.[11] However, an understanding of the observed processes requires also knowledge of the energy changes of the reactions. These can be obtained by theoretical methods,[11] but experimental data, such as those obtained by ion equilibria[7] and the present work, can provide useful checks and insights.

The binding energies within charged salt clusters and the energies of hydration of these species find applications in sometimes surprisingly different areas. For example, the salt cluster data are of importance in protein analysis by ESIMS. Salt adducts to the charged proteins occur as an undesired process integral to the ESI mechanism by which the proteins are transferred to the gas phase. The removal of these adducts by thermal dissociation is possible but depends on the strength of the bond between the charged side chain and the salt.[12] The magnitudes of the binding energies allow predictions to be made as to which salts in the solution will lead to undesirably strong bonded adducts that might be difficult to remove by thermal dissociation.[12]

Experimental and Theoretical Methods

(a) Experimental Details. Equilibrium Measurements. The experimental determinations of the equilibrium constants of the hydration reactions of the $(MX)_mM^+$ ions were performed with an apparatus that has been described.[13] The reactant $(MX)_mM^+$ ions were obtained by electrospray from a silica capillary, 0.1 mm internal diameter (i.d.), 0.25 mm o.d., and some 3 cm long, that terminated with a stainless capillary to which a positive voltage of 4 kV was applied. The solution was supplied to the metal capillary by a motor-driven syringe at a rate of 1 μL/min. The solution contained 10 mmol/L of the MX salt in methanol. Some of the spray, after passing through a dry nitrogen gas counter current, enters a transfer capillary at 30 V that leads to a fore-chamber where the ions are exposed to an electric field that deflects them toward an orifice leading to a reaction-equilibration chamber. The ions that enter this chamber are exposed to a weak electric field so that they drift at very low drift velocities to the vicinity of a small

(3) (a) Dalleska, N. F.; Tjelta, B. L.; Armentrout, P. B. *J. Phys. Chem.* **1994**, *989*, 4191−4195. (b) Marinelli, P. J.; Squires, R. R. *J. Am. Chem. Soc.* **1989**, *111*, 4101−4103. (c) Dzidic, I.; Kebarle, P. *J. Phys. Chem.* **1970**, *74*, 1466−1474. (d) Payzant, J. D.; Cunningham, A. J.; Kebarle, P. *Can. J. Chem.* **1973**, *51*, 3242−3249.
(4) (a) Davis, A. V.; Zanni, M. T.; Weinkauf, R.; Neumark, D. M. *Chem. Phys. Lett.* **2002**, *353*, 455−458. (b) Ayotte, P.; Weddle, G. H.; Johnson, M. A. *Chem. Phys.* **1999**, *110*, 7129−7132. (c) Choi, J. H.; Kuwata, K. T.; Cao, Y. B.; Okumura, M. *J. Phys. Chem.* **1998**, *102*, 503−507. (d) Markovich, G.; Pollack, S.; Giniger, R.; Cheshnovsky, O. *J. Chem. Phys.* **1994**, *101*, 9344−9353. (e) Hiraoka, K.; Mizuse, S.; Yamabe, S. *J. Phys. Chem.* **1988**, *92*, 3943−3952. (f) Arshadi, M.; Yamdagni, R.; Kebarle, P. *J. Phys. Chem.* **1970**, *74*, 1475−1482.
(5) (a) Hashimoto, K.; Morokuma, K. *J. Am. Chem. Soc.* **1994**, *116*, 11436−11443. (b) Bauschlicher, C. W.; Langhoff, S. R.; Patridge, H.; Rice, J. E.; Komornicki, A. *J. Chem. Phys.* **1991**, *95*, 5142−5148.
(6) (a) Lee, H. M.; Kim, D.; Kim, K. S. *J. Chem. Phys.* **2002**, *116*, 5509−5520. (b) Vila, F. D.; Jordan, K. D. *J. Phys. Chem. A* **2002**, *106*, 1391−1397. (c) Chen, H. Y.; Sheu, W. S. *J. Am. Chem. Soc.* **2000**, *122*, 7534−7542. (d) Gai, H. D.; Schenter, G. K.; Dang, L. X.; Garrett, B. C. *J. Chem. Phys.* **1996**, *105*, 8835−8841. (e) Serxner, D.; Dessent, C. E. H.; Johnson, M. A. *J. Chem. Phys.* **1996**, *105*, 7231−7234.
(7) Zhang, Q.; Carpenter, C. J.; Kemper, P. R.; Bowers, M. T. *J. Am. Chem. Soc.* **2003**, *125*, 3341−3352.
(8) Fenn, J. B.; Mann, M.; Meng, C. K.; Wong, S. K.; Whitehouse, C. *Science* **1989**, *246*, 64−71.
(9) Blades, A. T.; Jayaweera, P.; Ikonomou, M. G.; Kebarle, P. *J. Chem. Phys.* **1990**, *92*, 5900−5906.
(10) (a) Anacleto, J. F.; Pleasance, S.; Boyd, R. K. *Org. Mass Spectrom.* **1992**, *27*, 660−666. (b) Friedrich, J.; Weis, P.; Kaller, J.; Whetten, R. L.; Kappes, M. M. *Eur. Phys. J. D* **1999**, *9*, 269−272.
(11) Gregoire, G.; Mons, M.; Dimicoli, I.; Dedonder-Lardeux, C.; Jouvet, C.; Martrenchard, S.; Solgadi, D. *J. Chem. Phys.* **2000**, *112*, 8794−8805.
(12) Peschke, M.; Verkerk, U. H.; Kebarle, P. *J. Am. Soc. Mass Spectrom.*, in press.
(13) Blades, A. T.; Klassen, J. S.; Kebarle, P. *J. Am. Chem. Soc.* **1996**, *118*, 12437−12442.

orifice that leads to the pumped vacuum housing of a quadrupole mass spectrometer (see Figure 1 in Blades et al.[13]). The potential drop used in the drift region of the reaction-equilibration chamber was 5 V in all hydration equilibria determinations except for hydration of the MXM^+ by the first water molecule. These required longer equilibration times, and for these equilibria potentials of 2−4 V were used.

The fore-chamber and reaction chamber are maintained at a desired total pressure of N_2 bath gas in the 10 Torr range. The bath gas contains also a known partial pressure of the neutral reagent, H_2O, in the milli-Torr range. The fore-chamber and reaction chamber are located in a copper block whose temperature is controlled to within 0.2 °C during a given experiment. The ions are hydrated in the reaction chamber and reach equilibrium before entering the vacuum chamber leading to the mass spectrometer. Each successive hydration equilibrium was determined over a 40−70 °C temperature range at partial pressures of H_2O from 1 to 300 mTorr in N_2 bath gas.

Mass Spectra of Unhydrated, Magic Ions from NaCl Solutions. A Mariner Biospectrometry workstation (TOF, PerSeptive Biosystems, Framingham, MA) was used. This is a reflectron time-of-flight (TOF) mass spectrometer. The nanospray tips were positioned ∼1−2 mm from the sampling capillary, operated at a temperature of 35 °C. A spray voltage between 900 and 1100 V was applied. Depending on the CID voltage, the spray current was kept around 180 nA by adjusting the spray voltage. A counter flow of nitrogen (curtain gas) with a flow rate of 2.2 L min^{-1} was applied. The collision gas is thus N_2. The electric field and pressure in the interface region where the collision activation occurs are not well defined. In general, large pressure gradients happen to coincide with large field gradients. This results in a very large number of collisions of each ion with gas molecules such that the ion activation probably resembles that occurring under ion drift conditions. The mass spectra were obtained with a 10^{-2} M solution of NaCl in water by accumulating and averaging some 50 spectra, each 3 s per spectrum.

(b) Theoretical Calculations. All calculations were performed with Gaussian94.[14] The B3LYP density functional was the method of choice since it has previously shown excellent agreement with experimental metal cation and halide anion hydration results.[15] For Na, O, and H the 6-311++G(d,p) basis set was used. For iodine a number of basis sets were tried:[16a] 6-311G**,[16b] Stuttgart RLC ECP,[16c] Sadlej pVTZ,[16d] and a modified SDB-aug-cc-pVTZ[16e] basis set. All four agreed to within 0.5 kcal/mol on the monohydration energy of $NaI-H_2O$. Because the 6-311G** basis set was the easiest one to work with (not as fast as the effective core potential (ECP) basis sets but with analytical derivatives for the normal vibrational frequency calculations), it was chosen for all other calculations, except where indicated.

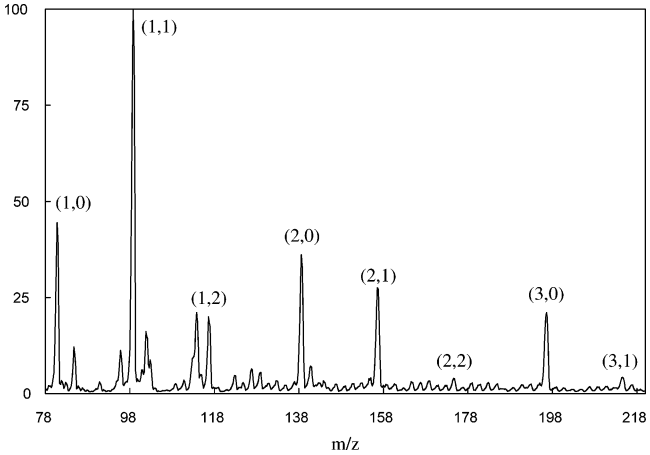

Figure 1. Observed ion intensities of $(NaCl)_mNa(H_2O)_n^+$ ions at equilibrium with 14 mTorr of water vapor at a temperature of 130 °C. Values of (m,n) are given above peaks. The results demonstrate that the degree of hydration decreases with increasing values of m. The spectra were obtained with monoisotopic ^{35}Cl.

The potential energy surface (PES) of $NaINa-H_2O^+$ was tested extensively to ascertain whether the ion−dipole optimized linear arrangement or a bent geometry with a hydrogen−I interaction was lower in energy. These calculations showed that the PES is very flat, with the geometries differing by less than 0.5 kcal/mol for the water in a linear or bent configuration but also for NaINa bending to allow more favorable polarization interactions with iodine. It is therefore fair to assume, as was done by other authors,[17] that under thermal conditions the equilibrium structure is linear.

For $H_2O-NaINa-H_2O^+$ the PES also was quite flat, and surprisingly, neither the linear arrangement with both hydrogen pairs in the plane, nor the arrangement with the pairs at 90° angles to each other, was a minimum. The structure that had no imaginary frequencies showed the two pairs at an angle of approximately 55° to each other. However, because the energy differences were less than 0.01 kcal/mol, under thermal conditions the hydrogen pair motion would be that of a free or hindered rotor. Nevertheless, the frequency result was used in order to avoid the more complicated analysis to determine the free or hindered rotor contribution to the entropy. The results agree very well with experiment and show that, for this system, such errors are either small or cancel. The frequencies (in cm^{-1}) are as follow: $NaINa^+$, 22.4, 22.4, 194.2, 217.2; $NaINa{\cdot}H_2O^+$, 19.1, 19.4, 36.9, 42.0, 135.4, 214.7, 312.0, 363.6, 423.8, 1667, 3803, 3883; $NaINa{\cdot}2H_2O^+$, 15.6, 15.7, 35.3, 36.4, 40.9, 41.3, 54.3, 127, 157, 313, 313.4, 358.5, 360, 420.7, 421, 1666, 1666, 3804, 3804, 3884, 3884.

Results and Discussion

(a) Description of Results. Shown in Figure 1 is the mass spectrum observed when a 10 mM solution of $Na^{35}Cl$ in methanol was sprayed and the reaction chamber at 130 °C contained 11 Torr buffer gas and 14 mTorr H_2O vapor. The $Na(NaCl)_m(H_2O)_n^+$ cluster peaks are identified by the values (m,n) shown beside the peaks. The major ions observed under these conditions were due to $Na(H_2O)_n^+$. These ions are not shown in Figure 1. The observed relative peak heights of the $Na(NaCl)_m(H_2O)_n^+$ ions predict the relative stability of the hydrates because the ions have reached hydration equilibrium

(14) Frisch, M. J.; Trucks, G. W.; Schlegel, H. B.; Gill, P. M. W.; Johnson, B. G.; Robb, M. A.; Cheeseman, J. R.; Keith, T.; Petersson, G. A.; Montgomery, J. A.; Raghavachari, K.; Al-Laham, M. A.; Zakrzewski, V. G.; Ortiz, J. V.; Foresman, J. B.; Cioslowski, J.; Stefanov, B. B.; Nanayakkara, A.; Challacombe, M.; Peng, C. Y.; Ayala, P. Y.; Chen, W.; Wong, M. W.; Andres, J. L.; Replogle, E. S.; Gomperts, R.; Martin, R. L.; Fox, D. J.; Binkley, J. S.; Defrees, D. J.; Baker, J.; Stewart, J. P.; Head-Gordon, M.; Gonzalez, C.; Pople, J. A. *Gaussian 94*, Revision D.3; Gaussian, Inc., Pittsburgh, PA, 1995.

(15) (a) Smith B. J.; Radom L. *Chem. Phys. Lett.* **1994**, *231*, 345−351. (b) Soliva R.; Orozco M.; Luque F. J. *J. Comput. Chem.* **1997**, *18*, 980−991. (c) Bogdanov B.; Peschke M.; Tonner D. S.; Szulejko J. E.; McMahon T. B. *Int. J. Mass Spectrosc.* **1999**, *187*, 707−725. (d) Peschke M.; Blades A. T.; Kebarle P. *Int. J. Mass Spectrosc.* **1999**, *187*, 685−699. (e) Scott A. P.; Radom, L. *J. Phys. Chem.* **1996**, *100*, 16501−16513. (f) East, A. L. L.; Radom, L. *J. Chem. Phys.* **1997**, *106*, 6655−6674.

(16) (a) Basis sets were obtained from the Extensible Computational Chemistry Environment Basis Set Database, Version 1.0, as developed and distributed by the Molecular Science Computing Facility, Environmental and Molecular Sciences Laboratory, which is part of the Pacific Northwest Laboratory, P.O. Box 999, Richland, WA 99352, and funded by the U.S. Department of Energy. The Pacific Northwest Laboratory is a multi-program laboratory operated by Battelle Memorial Institute for the U.S. Department of Energy under contract DE-AC06-76RLO 1830. Contact David Feller, Karen Schuchardt, or Don Jones for further information. (b) Glukhovtsev M. N.; Pross A.; McGrath M. P.; Radom L. *J. Chem. Phys.* **1995**, *103*, 1878−1885. (c) Bergner A.; Dolg M.; Kuechle W.; Stoll H.; Preuss, H. *Mol. Phys.* **1993**, *80*, 1431−1441. (d) Sadlej A. J. *Theor. Chim. Acta* **1992**, *81*, 339−354. (e) Relativistic ECP definitions were taken from ref 3c; basis set exponents and contractions were taken from Martin J. M. L.; Sundermann A. *J. Chem. Phys.* **2001**, *114*, 3408−3420. f-orbital definitions were deleted since Gaussian94 had problems with derivatives if they were defined.

(17) Vacek, G.; DeLeeuw, B. J.; Schaeffer, H. F. *J. Chem. Phys.* **1993**, 98, 8704−8709.

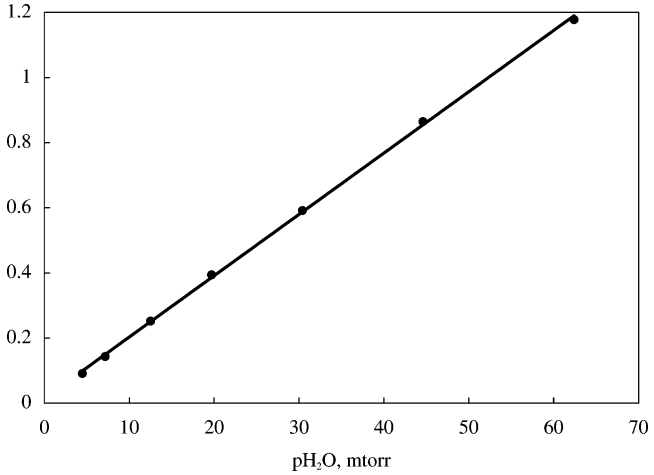

Figure 2. Plot of ion intensity ratio $I(NaClNa{\cdot}2H_2O)^+/I(NaClNa{\cdot}H_2O)^+$ versus partial pressure of H_2O, leading to a straight line, with slope equal to $K_{n-1,n}$, that goes through the origin as expected from eq 2. Temperature, 127 °C.

at the stated experimental conditions. The drift time (equal to the reaction time) for a singly charged ion such as n-$C_4H_9NH_3^+$, under the bath gas pressure and reaction temperature conditions used, is approximately 150 μs (see Peschke et al.[18]). This time and the H_2O partial pressure used are sufficient for the attainment of the hydration equilibria. The degree of hydration indicated by the intensities decreases as m in $Na(NaCl)_m(H_2O)_n^+$ increases. Thus, the (m,n) peak (1,1) is very much higher than the (1,0) peak, while the (3,1) peak is very much smaller than the (3,0) peak, and that means that the hydration exoergicity of the $m = 1$ ion is much greater than that of the $m = 3$ ion. This effect was first observed in the previous work with NaI by Zhang et al.[7]

Below we consider the equilibria of the $m = 1$ ions,

$$NaClNa(H_2O)_{n-1}^+ + H_2O \rightleftharpoons NaClNa(H_2O)_n^+ \quad (n-1,n) \quad (1)$$

for which the equilibrium constant is

$$K_{n-1,n} = p(NaClNa(H_2O)_n^+)/p(NaClNa(H_2O)_{n-1}^+)p(H_2O) \quad (2)$$

In the mass spectrometric determinations of $K_{n-1,n}$, the ratio of the partial pressures of the ions is replaced by the observed ion intensity ratio.[13] The ion count ratio $I_n/I_{n-1} = I_2/I_1$ is shown in Figure 2, plotted versus the $p(H_2O)$ used. The straight line obtained, which goes through the origin and whose slope is equal to $K_{1,2}$, as predicted by eq 2, demonstrates the validity of the method used for the determination of the equilibrium constants. The ion count ratio, I_n/I_{n-1}, in Figure 2 changes from ~0.1 to 1.2. We have found in previous work that this spread of ratios leads to the most consistent data in previous work, and data obtained in this range were used for all the determinations reported in the present work. Equilibrium constants obtained from the slope of the straight line in such plots, at different constant temperatures, were used in van't Hoff plots (see Figures 3−5) for $NaINa^+$, $NaClNa^+$, and $NH_4INH_4^+$ to obtain the enthalpy and entropy change.

$$-RT \ln K_{n-1,n} = \Delta G_{n-1,n}^\circ = \Delta H_{n-1,n}^\circ - T\Delta S_{n-1,n}^\circ \quad (3)$$

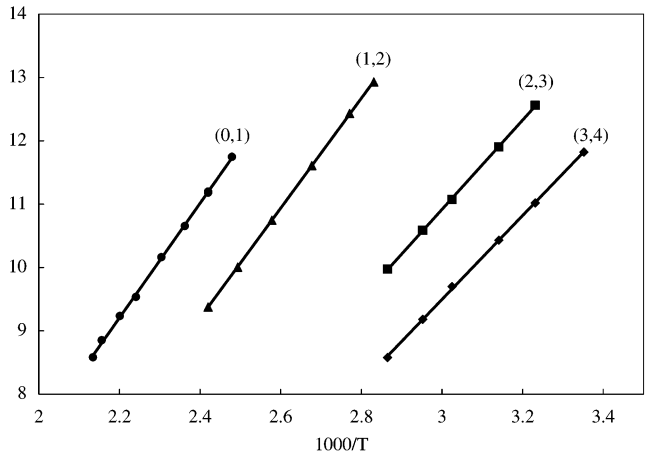

Figure 3. van't Hoff plots of equilibrium constants $K_{n-1,n}$ for hydration equilibria involving $NaINa^+$. Values of (n − 1,n) are given above the respective plots.

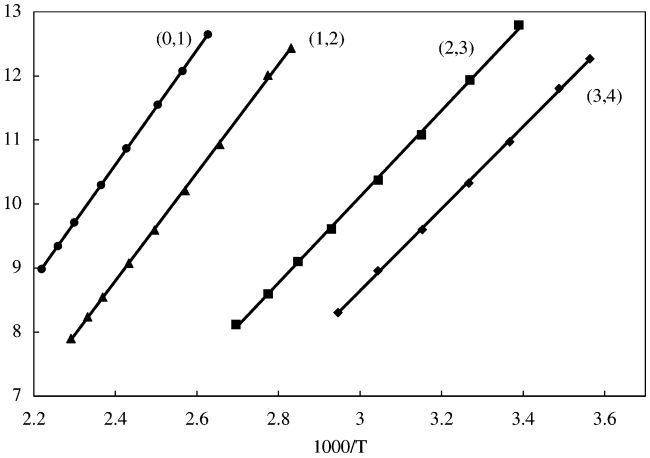

Figure 4. van't Hoff plots of equilibrium constants $K_{n-1,n}$ for hydration equilibria involving $NaClNa^+$. Values of (n − 1,n) are given above the respective plots.

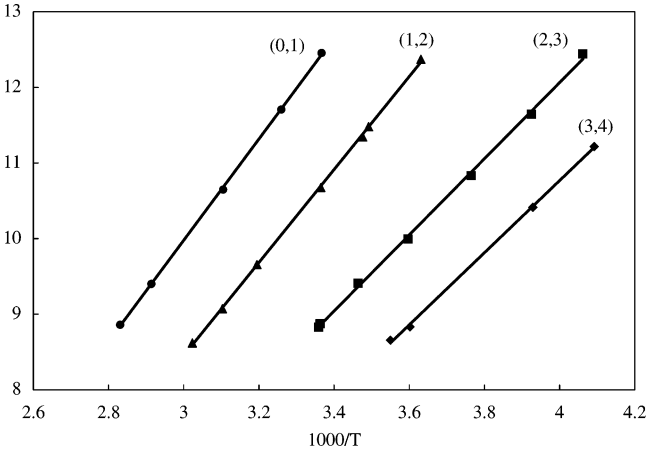

Figure 5. van't Hoff plots of equilibrium constants $K_{n-1,n}$ for hydration equilibria involving $NH_4INH_4^+$. Values of (n − 1,n) are given above the respective plots.

The thermodynamic data obtained from these and other plots that are not shown are summarized in Tables 1−3.

(b) Monohydration of MXM^+, Where M = Na and X = I, Br, Cl, F, NO_2, NO_3. The $\Delta H_{1,0}^\circ$ and $\Delta S_{1,0}^\circ$ values for the series where the positive ion Na^+ is the same and the X^- ions are changed are given in Table 1 for X = I and Table 2 for X

Table 1. Hydration Data[a] for $NaINa^+$

	$\Delta H_{n,n-1}^\circ$				$\Delta S_{n,n-1}^\circ$			
	experimental		theoretical		experimental		theoretical	
n								
1	18.0	(19.3)[b]	18.5[c] (19.0)[c]	(18.3)[b]	21.2	(22.2)[b]	22.4[c] (23.2)[c]	(22.0)[b]
2	17.2	(19.2)[b]	17.8[d] (18.2)[d]	(17.8)[b]	23.1	(28.0)[b]	23.3[d] (24.2)[d]	(27.6)[b]
3	14.0	(13.4)[b]		(13.6)[b]	20.4	(17.8)[b]		(20.5)[b]
4	13.2	(13.6)[b]		(13.5)[b]	20.6	(21.1)[b]		(32.5)[b]

[a] Data for reactions $NaINa(H_2O)_n^+ \rightleftharpoons NaINa(H_2O)_{n-1}^+ + H_2O$. All enthalpy values in kcal/mol, all entropies in $cal \cdot mol^{-1} \cdot K^{-1}$ valid for range shown in Figure 3. [b] Results from Table 1, Zhang et al.[7] The enthalpies in this reference are given for 0 K. However, the entropy changes are for the average temperature of the experiment,[7] i.e., below 400 K. [c] Theoretical values, present work, corrected to experimental temperature of 436 K. Values in parentheses are for 298 K. [d] Theoretical values, present work, corrected to experimental temperature of 393 K. Values in parentheses are for 298 K.

Table 2. Hydration Data for $NaXNa^+$, with X = Br, Cl, F, NO_2, NO_3[a]

	Br		Cl		F		NO_2		NO_3	
n	$\Delta H_{n,n-1}^\circ$	$\Delta S_{n,n-1}^\circ$	$\Delta H_{n,n-1}^\circ$	$\Delta S_{n,n-1}^\circ$	$\Delta H_{n,n-1}^\circ$	$\Delta S_{n,n-1}^\circ$	$\Delta H_{n,n-1}^\circ$	$\Delta S_{n,n-1}^\circ$	$\Delta H_{n,n-1}^\circ$	$\Delta S_{n,n-1}^\circ$
1	17.7	21.0	18.2	22.5	17.0	21.8	17.7	21.5	17.4	21.1
2	17.2	23.2	16.8	22.8	15.9	22.7	15.9	21.5	16.1	21.0
3			13.4	20.0						
4			12.7	21.1						

[a] Data for reactions $MXM(H_2O)_n^+ \rightleftharpoons MXM(H_2O)_{n-1}^+ + H_2O$. All enthalpy values in kcal/mol, all entropies in $cal \cdot mol^{-1} \cdot K^{-1}$.

Table 3. Hydration Data for (a) MIM^+ [a] and (b) M^+ [b]

	NH_4		Na		K		Rb		Cs	
n	$\Delta H_{n,n-1}^\circ$	$\Delta S_{n,n-1}^\circ$	$\Delta H_{n,n-1}^\circ$	$\Delta S_{n,n-1}^\circ$	$\Delta H_{n,n-1}^\circ$	$\Delta S_{n,n-1}^\circ$	$\Delta H_{n,n-1}^\circ$	$\Delta S_{n,n-1}^\circ$	$\Delta H_{n,n-1}^\circ$	$\Delta S_{n,n-1}^\circ$
					(a) For MIM^+					
1	13.3	20.1	18.0	21.2	13.1	20.1	12.2	19.6	11.3	20.0
2	12.2	19.9	17.2	23.1						
3	10.0	16.1	14.0	20.4						
4	9.5	16.5	13.2	20.6						
					(b) For M^+					
1	17.3	19.7	24.0	21.5	17.9	21.6	15.9	21.2	13.7	19.4

[a] Data for reactions $MIM(H_2O)_n^+ \rightleftharpoons MIM(H_2O)_{n-1}^+ + H_2O$. All enthalpy values in kcal/mol, all entropies in $cal \cdot mol^{-1} \cdot K^{-1}$. [b] All enthalpy values in kcal/mol, all entropies in $cal \cdot mol^{-1} \cdot K^{-1}$. These are literature data given for comparison. Values for alkali ions from Dzidic and Kebarle,[3c] values for NH_4^+ from Payzant et al.[3d]

= Br, Cl, F, NO_2, and NO_3. The experimental values in the tables are given not for the $(n-1,n)$ but for the reverse reaction $(n,n-1)$ because the $(n,n-1)$ values are positive numbers and this simplifies the discussion of the relative changes of the values. The $\Delta H_{1,0}^\circ$ values (Tables 1 and 2) are surprisingly similar, all falling between the limits 17 and 18.0 kcal/mol. Although the result of 18.2 kcal/mol for NaClNa is out of line, the other results indicate a monotonic increase from 17 to 18.0 kcal/mol from X = F to X = I. We believe that a larger experimental error of some 0.5 kcal/mol in the NaClNa determination is responsible for the deviation. The usual estimated error is 0.3 kcal/mol. The actual trend is probably more accurately predicted by the $\Delta G(400\ K)$ values, which are 8.3, 9.2, 9.3, and 9.5 kcal/mol from F to I. These show a large step between F and Cl which probably is due to the relatively large increase of the ionic radii from F to Cl.

The above results and the overall small upward trend from F to I are easily understood when one considers that the bonding of H_2O to the $NaXNa^+$ ions is largely electrostatic. Assuming that unit charges are located in the centers of the ions and using the Pauling radii[19] for the alkali and halide ions, and assuming that the alignment of Na−X−Na−O is linear, one obtains the results shown in Table 4. Only the interaction of the charges of the ions, assumed to be in the center of the ion, with the dipole and induced dipole of the water molecule were considered; i.e., the polarizability of the ions themselves was neglected. The results (Table 4) do provide a good illustration of the main electrostatic contributions to the bond energy, even though the calculation can be considered primitive. The $\Delta H_{1,0}^\circ$ bond energy trends observed in Tables 2 (F, Cl, Br) and 3 (I) are well reproduced by the electrostatic results that also show a very small change with the different X^- ions and a slight increase from F^- to I^-. The changes are small, which must be due to the dominant interaction of the permanent and induced dipoles of water with the adjacent Na^+ ion, which remains constant for the series. The bond energy is decreased by the repulsive interaction of the X^- ion with the dipole and an induced dipole of H_2O which is of opposing polarity (the induced dipole effect, which is expected to be small, was not included in the electrostatic calculations). The negative effect of X^-, which decreases with the size of X^-, is partially canceled by the weak, positive, i.e., bonding, interaction of the terminal Na^+ ion with the permanent and induced dipoles of the H_2O molecule. The Na^+ bonding interaction also decreases with the size of X^-.

The electrostatic results also predict bonding of H_2O to the neutral NaX. The bonds in $NaX-OH_2$ are not much weaker than the predicted $(NaXNa-H_2O)^+$ bonds because the electrostatic contribution of the remote Na in the $(NaXNa-H_2O)^+$ complex is rather small (see Table 4). More accurate values

(18) Peschke, M.; Blades, A. T.; Kebarle, P. *J. Am. Chem. Soc.* **2002**, *124*, 11519−11530.
(19) Pauling, L. *The Nature of the Chemical Bond*, 3rd ed.; Cornell University Press: Ithaca, NY, 1967; p 514.

Table 4. Bond Energy for $NaXNa^+-OH_2$ and $NaX-OH_2$ Predicted by Simple Electrostatic Calculations[a]

X^-	R/Å[b]	$E_D(Na^+)$[c]	$E_D(X^-)$[d]	$E_D(Na^+)$[e]	$E_P(X^-)$[f]	$E_T(NaXNa^+)$[g]	$E_T(NaX)$[h]
F^-	1.36	14.72	−4.35	2.05	0.28	15.67	13.62
Cl^-	1.81	14.72	−3.67	1.63	0.20	15.93	14.30
Br^-	1.91	14.72	−3.54	1.55	0.19	15.98	14.43
I^-	2.16	14.72	−3.24	1.38	0.16	16.11	14.73[i]

[a] The results for the bond energies of water to $NaXNa^+$ and NaX are only approximate and are given to illustrate the approximate contributions of the interaction of the water dipole and polarizability with the $Na^+X^-Na^+$ charges. All energy values are in kcal/mol. [b] Pauling radius of X^-. A Pauling radius of 0.95 Å was used for Na^+. A radius of 1.8 Å was used for the H_2O molecule. [c] Water dipole interaction with nearest Na^+. A water dipole $\mu = 1.85$ D was used. [d] Water dipole interaction with X^-. [e] Water dipole interaction with remote Na^+. [f] Polarizability interaction with charge of nearest Na^+. $\alpha(H_2O) = 1.48$ Å^3. [g] Sum of all interaction energies. Bond energy of hydration of H_2O to MXM^+. [h] Bond energy of hydration of H_2O to NaX. [i] The theoretical DFT calculations lead to 14.2 kcal/mol (Zhang et al.[7]) and 13.9 kcal/mol (present work). The close agreement of the electrostatic result, 14.7 kcal/mol, with the theoretical results must be fortuitous. Thus, the structures predicted by the theoretical calculations are quite different[7] from the linear alignment, assumed in the simple electrostatic calculation.

for the bond energy of NaI with H_2O are available from theoretical calculations. Thus, Hynes and co-workers[20] cite a value of 16 kcal/mol based on Monte Carlo simulations. The ab initio result in the present work is $\Delta E = 13.9$ kcal/mol (see Theoretical Calculations), while the ab initio results of Zhang et al.[7] led to a value of 14.2 kcal/mol.

(c) Monohydration of MXM^+, Where X = I and M = NH_4, Na, K, Rb, Cs. The experimentally obtained $\Delta H_{1,0}°$ values for the MIM^+ hydrates given in Table 3 show a strong dependence on the nature of the M^+ ion. It is seen that the values for MIM^+ follow quite closely the changes observed for the naked M^+ ions, but are somewhat smaller. A plot (not shown) of $\Delta H_{1,0}(MIM^+)$ versus $\Delta H_{1,0}(M^+)$ gives a monotonic increase from Cs to Na, although the values for NH_4 and K, which are close, exhibit a small reversal. It is possible that the M^+ hydration values in the original references,[3c,d] that lead to $\Delta H_{1,0}(K^+) > \Delta H_{1,0}(NH_4^+)$, are in error. The general trend from Cs to Na could have been fully anticipated from the electrostatic predictions discussed in the previous section. Because the M^+ ion adjacent to the H_2O provides the dominant electrostatic interaction, a change of the M^+ ion should lead to changes in the $\Delta H_{1,0}°$ values for MIM^+ that are close to the $\Delta H_{1,0}°$ for the hydration of the naked M^+ ions. However, they should be smaller, due to the repulsive interaction of the negative ion X^-, whose effect is larger than the bonding interaction of the remote Na^+.

(d) Successive (n,$n-1$) Hydration Energies of MIM^+ Ions. Experimental values for the successive hydration energies for $NaINa^+$ are given in Table 1. Determinations for $NaINa(H_2O)_n^+$ extending to higher values of n have been reported by Zhang et al.[7] Both data sets show that the change of $\Delta H_{n,n-1}°$ values with n occurs stepwise. Thus, $\Delta H_{1,0}°$ and $\Delta H_{2,1}°$ are very similar, and then a relatively big drop occurs between $\Delta H_{2,1}°$ and $\Delta H_{3,2}°$, and then $\Delta H_{3,2}°$ and $\Delta H_{4,3}°$ are very similar again. This is an expected result when two equivalent sites of hydration are present in the molecule and when these two sites are separated by some distance from each other. The effect was first observed in the hydration of diprotonated alkyl diamines,[13] $NH_3(CH_2)_pNH_3^{2+}$. The corresponding entropy changes need not be coupled in the same manner. Changes of rotational symmetry numbers can be present, which lead to additional trends, as was found to be the case for the diamines.[13]

The agreement between the present experimental data and those of Zhang et al.[7] is mostly within 1 kcal/mol for the ΔH values and 2 cal·mol^{-1}·K^{-1} for the ΔS values, which is good for determinations with different apparatus in two different laboratories. Furthermore, Zhang's enthalpy values are given for 0 K, and the heat capacity change to the temperature for our enthalpies is on the order of 0.5−1 kcal/mol.

Table 5. Individual Entropy Contributions at 298 K As Evaluated from Theoretical Calculations[a]

	S(transl.)	S(rot.)	S(vib.)	S(tot.)[c]
$NaINa^+$ (linear)	41.4	17.4 (19.3)[b]	17.0	75.8
$NaINa^+$ (bent)	41.4	25.2	10.3	76.9
$NaINa-OH_2^+$	41.6	23.7 (24.6)[b]	32.2	97.5
$H_2O-NaINa-OH_2^+$	41.9	24.0 (24.9)[b]	52.6	118.5

[a] From B3LYP density functional calculations, see Experimental and Theoretical Calculations section. All entropies are given in cal·mol^{-1}·K^{-1}. [b] Theoretical data from Zhang et al.[7] for temperatures below 400 K. [c] Total entropy based on theoretical calculations, this work. Results given predict the values for dehydration entropy changes: $\Delta S°_{2,1} - \Delta S°_{1,0} = 0.8$ cal·mol^{-1}·K^{-1} ($NaINa^+$ linear) and −0.3 cal·mol^{-1}·K^{-1} ($NaINa^+$ bent).

The theoretical predictions for the ΔH and ΔS values are also relatively close. However, there are also some discrepancies between the ΔH and ΔS experimental and theoretical values for the first two hydration steps that need some comment. The experimental difference $\Delta H_{1,0}° - \Delta H_{2,1}° = 0.8$ kcal/mol (present results Table 1). A similar difference is indicated by the theoretical calculations of the present work and those of Zhang et al.[7] (see Table 1). However, Zhang et al.[7] have an experimentally determined difference of only 0.1 kcal/mol, which seems too small considering the proximity of the two Na^+ ions.

The experimental entropy differences $\Delta S_{2,1}° - \Delta S_{1,0}° = 0.9$ cal·mol^{-1}·K^{-1} (present work) and 5.8 cal·mol^{-1}·K^{-1} (Zhang et al.), while the theoretical calculations predict 0.8 cal·mol^{-1}·K^{-1} (NaINa linear, present work) and 5.6 cal·mol^{-1}·K^{-1} (Zhang et al., Table 1). The large entropy difference for the successive hydration reactions in the results of Zhang et al. is surprising. Large differences have been observed experimentally for the alkyl diamines,[13] $NH_3(CH_2)_pNH_3^{2+}$ (see above), but in that case three specific (hydrogen) bonding sites are present on each $-NH_3^+$ group, and these lead, as mentioned above, to rotational entropy differences. Zhang et al.[7] attribute the large difference obtained in their results to the small value of the rotational entropy of the linear S(NaINa) (see S_{rot} values in Table 5). However, according to our theoretical results, the linear $NaINa^+$ has some very soft vibrational modes which fully compensate for the rotational entropy difference. The data in Table 5 make it clear that the different theoretical entropy predictions must be due to differences of the vibrational frequencies used in the calculations. Although the basis sets are very similar, arguably the basis set of Zhang et al. could be the better one because

(20) Peslherbe, G. H.; Ladanyi, B. M.; Hynes, J. T. *J. Phys. Chem. A* **1998,** *102*, 4100−4110.

it includes relativistic correction for the I atom. The vibrational frequencies for the mono- and dihydrate include several very low frequencies and some that are lower than 20 cm^{-1}, particularly for the dihydrate. These lead to large vibrational entropy contributions that may be unreliable because the internal modes that they often represent, such as anharmonic vibrations and hindered internal rotations, cannot be accurately evaluated from the predicted vibrational frequencies.[15e,f] Therefore, the likely source for the different theoretical results of Zhang et al. and the present work could be the use of modified frequencies for the soft vibrations. Such procedures have been discussed by Radom and co-workers.[15e] In the present vibrational entropy calculations, the frequencies were used without change. Zhang et al. provide a set of frequencies for $NaINa^+$ and the hydrates in their Supporting Information. These were used by them for phase space calculations. An evaluation of the vibrational entropies with these frequencies in the present work, when combined with the rotational and translational entropies of Zhang et al., leads to $\Delta S_{2,1}^\circ - \Delta S_{1,0}^\circ \approx 0.1$ cal mol^{-1} at temperatures close to 300 K. This result is very close to the present results, 1.9 experimental and 0.9 cal·mol^{-1}·K^{-1} theoretical (see Table 1). Because the Zhang et al. reported theoretical $\Delta S_{2,1}^\circ - \Delta S_{1,0}^\circ = 5.6$, it appears that they did use modified soft frequencies, even though this was not mentioned explicitly and no indication was given of the specific changes that were made.

A comparison of our reported experimental and theoretical $\Delta S_{n,n-1}^\circ$ values for $n = 3$ and $n = 4$, and those reported by Zhang et al. (see Table 1), shows that agreement of all the results is present for $n = 3$. For $n = 4$, there is good agreement between the experimental results, which indicate ~21.0 cal·mol^{-1}·K^{-1}, while the theoretical value reported by Zhang et al. is 32.5 cal·mol^{-1}·K^{-1}. This suggests an error in the theoretical $\Delta S_{4,3}^\circ$, which is not surprising considering the expected presence of many soft frequencies in the higher hydrates. This example illustrates that accurate experimental results can be of great value to the development of theoretical methods for the evaluation of the entropy of such complexes.

(e) Hydration of $(MX)_mM^+$ Ions and Particularly Magic $(MX)_mM^+$ Ions. It was shown in section 1 and Figure 1 that the hydration energies $\Delta G_{n,n-1}^\circ$ decrease as m in $(MX)_mM^+$ increases. Zhang et al.,[7] who made much more detailed studies of the hydration of the $NaINa^+$ and $(NaI)_2Na^+$ ions, have also shown that the hydration energies $\Delta H_{n,n-1}^\circ$ and $\Delta G_{n,n-1}^\circ$ of the $(NaI)_2Na^+$ ions are lower. As m increases, one might expect some clusters which are significantly more stable to be present at higher intensities, and one might expect that these magic ion clusters will have lower hydration energies.

Here we consider results for the hydration of the cluster ions obtained with NaCl solutions. With NaCl, magic numbers have been observed[21,22] at $(NaCl)_mNa^+$ and $(NaCl)_mCl^-$ with $m = 4$, 13, and 22. Hydration equilibrium results with the lower mass range apparatus used for the hydration work could be obtained only for $(NaCl)_mNa^+$ of the magic number $3 \times 3 \times 1$ ($m = 4$) and the neighboring non-magic ions, $m = 3$ and $m = 5$. The

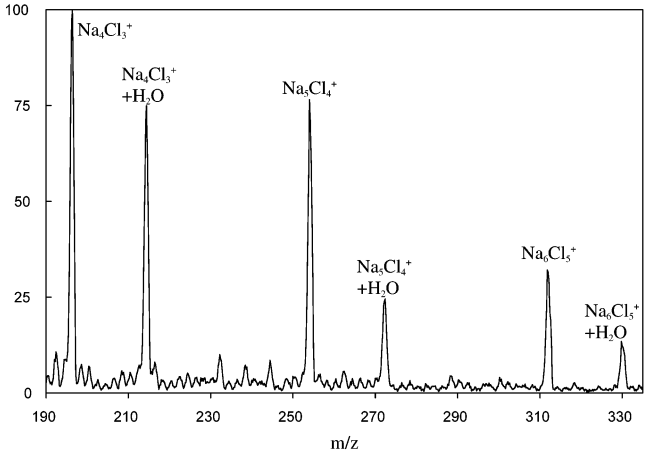

Figure 6. Ion intensities observed for $Na^{35}Cl$ ions when in hydration equilibrium at 352 K temperature. The $Na_5Cl_4^+$ ion, $Na(NaCl)_4^+$, that is proposed to have the structure $3 \times 3 \times 1$ (see text) is less hydrated than the adjacent mass ions, $Na_4Cl_3^+$ and $Na_6Cl_5^+$. This suggests that the structure of the $3 \times 3 \times 1$ ion is more stable than those of the adjacent ions.

Table 6. Hydration Free Energy, $\Delta G_{1,0}^\circ$(352 K) for Some $(NaCl)_mNa^+$ Ions[a]

$NaClNa^+$	$(NaCl)_2Na^+$	$(NaCl)_3Na^+$	$(NaCl)_4Na^+$	$(NaCl)_5Na^+$
10.2	9.4	8.1	7.3	7.9

[a] ΔG° values in kcal/mol.

$\Delta G_{1,0}^\circ$ values are given in Table 6. The $\Delta G_{1,0}^\circ$ values for $m = 1$ and $m = 2$ obtained at the same temperature, 352 K, are also given for comparison. In general, as expected, the $\Delta G_{1,0}^\circ$ values decrease as m is increased; however, the $\Delta G_{1,0}^\circ$ value for $m = 4$ is special because it is lower than that for $m = 3$ and $m = 5$. This special behavior is directly observable in the mass spectrum of the ions $m = 3$, 4, and 5 at hydration equilibrium conditions, shown in Figure 6. It is quite obvious that the intensity ratio monohydrate/naked ion is lowest for the $m = 4$ species.

Reliable structures and energies for $(NaCl)_mNa^+$ for $m = 2-14$ have been published by Phillips, Conover, and Bloomfield.[23] These are based on the Coulomb interactions of the constituent ions, the repulsion due to overlap of the wave functions of the ions (the Born−Mayer potential), and an ion polarizability α for each ion attributed to Rittner.[24] Monte Carlo methods were also employed for searches of low-energy isomers. The energies for small clusters up to $m = 4$ have been calculated also by ab initio methods and found[25] to be in good agreement with the energies obtained with the semiempirical method.[23] The experiments and the theory show that the alkali halide clusters tend to form face-centered-cubic lattice fragments. These face-centered cuboids exhibit complete surface terraces whenever possible. Recent results reported by Jarrold and co-workers,[22] based on high-resolution ion mobility measurements that provide information on the structures of the ions, have provided convincing evidence that such structural transitions to more stable configurations occur by surface migration of single ions even at ambient temperatures.[22b] The $3 \times 3 \times 1$ $(NaCl)_4Na^+$ ion represents the lowest form of a complete face-centered cuboid surface. Its structure is an almost flat umbrella with an Na^+ ion at the tip.[22a,23]

(21) (a) Pflaum, R.; Sattler, K.; Recknagel, E. *Chem. Phys. Lett.* **1987**, *138*, 8−12. (b) Friedrich, J.; Weis, P.; Kaller, J.; Whetten, R. L.; Kappes, M. M. *Eur. Phys. J. D* **1999**, *9*, 269−272.
(22) (a) Dugourd, P.; Hudgins, R. R.; Jarrold, M. F. *Chem. Phys. Lett.* **1997**, *267*, 186−192. (b) Hudgins, R. R.; Dugourd, P.; Tennenbaum, J. M.; Jarrold, M. F. *Phys. Rev. Lett.* **1997**, *78*, 4213−4216.
(23) Phillips, N. G.; Conover, C. W. S.; Bloomfield, L. A. *J. Chem. Phys.* **1991**, *94*, 4980−4987.
(24) Rittner, E. S. *J. Chem. Phys.* **1951**, *19*, 1030−1035.
(25) Weis, P.; Ochsenfeld, C.; Ahlrichs, R.; Kappes, M. M. *J. Chem. Phys.* **1992**, *97*, 2553−2560.

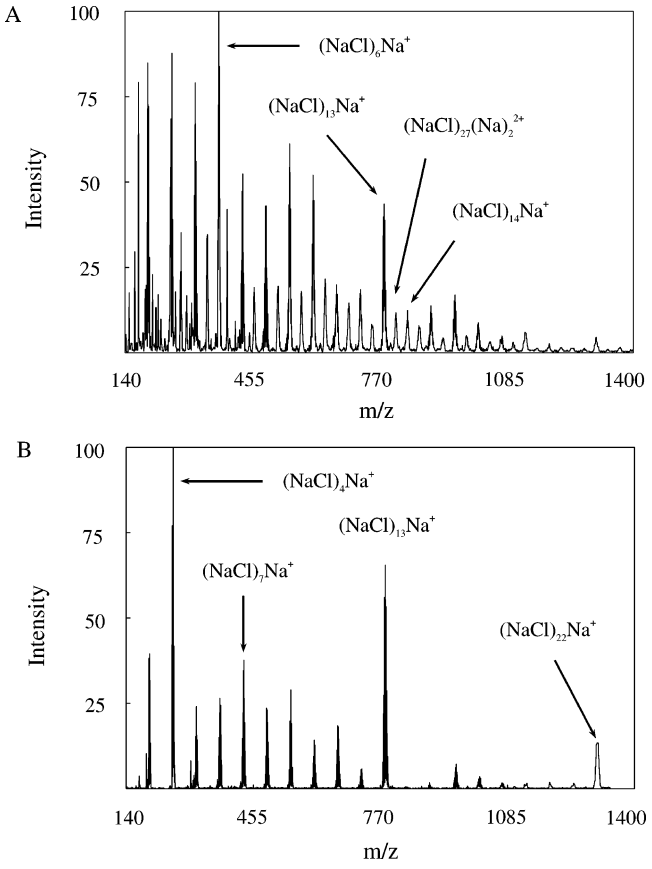

Figure 7. Ion intensities observed with a time-of-flight mass spectrometer and nano-electrospray of aqueous NaCl (natural isotope distribution) at two different ion drift potentials in spectrometer interface. (A) At very low or no activation, 50 V, the magic ions $(NaCl)_mNa$, with $m = 4$, 13, and 22, appear to be not prominent. (B) At high activation, 450 V, magic ions with $m = 4$, 13, and 22 are very prominent.

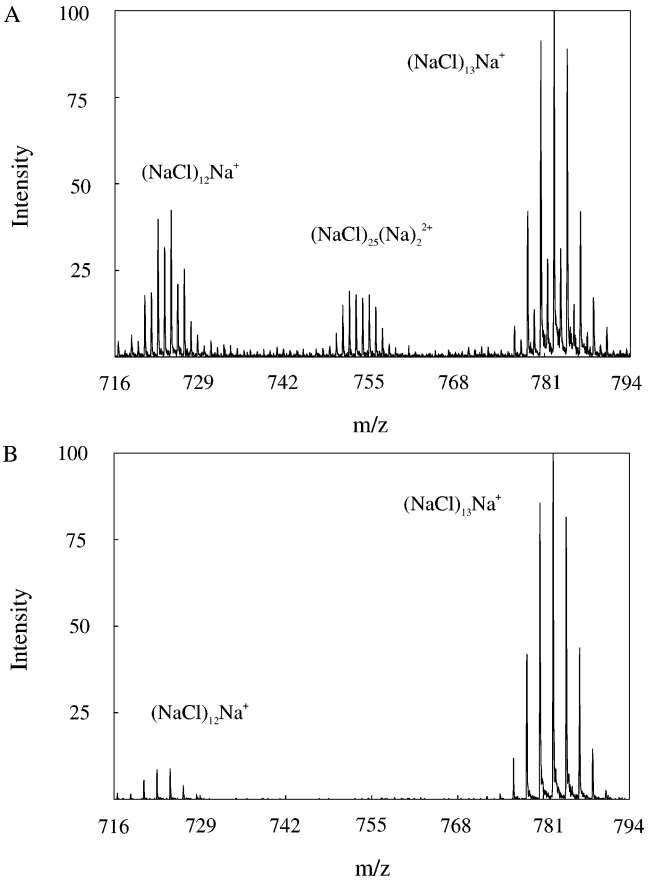

Figure 8. Expanded mass scale spectra at same conditions as in Figure 7. (A) At very low activation, 50 V. (B) At high activation, 450 V. At high activation, the magic ion group $(NaCl)_{13}Na^+$ is the most prominent ion group. The peaks in that group are spaced two mass units apart. This is due to the presence of the natural isotopes ^{35}Cl and ^{37}Cl. At low activation, the magic ion group is still prominent, but one needs to consider the presence of doubly charged ions. Doubly charged ions $(NaCl)_{2m}Na_2^{2+}$ and $(NaCl)_{2m+1}Na_2^{2+}$, such as $(NaCl)_{25}(Na)_2^{2+}$, are clearly visible. The doubly charged ions can be recognized by the single mass spacing between the chlorine isotope peaks that result from the presence of pairs of ^{35}Cl and ^{37}Cl in the doubly charged ion. The $(NaCl)_{2m}Na_2^{2+}$ ions overlap with the $(NaCl)_mNa^+$ ions. Thus, the ion designated in panel A as $(NaCl)_{12}Na^+$ is mostly due to doubly charged $(NaCl)_{24}Na_2^{2+}$ ions, while the magic ion designated as $(NaCl)_{13}Na^+$ contains only some 25% of doubly charged ions and is thus still a magic ion. The disappearance of the doubly charged ions at high activation demonstrates that the magic ions are produced by decomposition of both doubly and singly charged higher mass ions.

(f) Are the Magic Ions Observed with Electrospray Due to Ion Clusters Present in the Saturated Solution of the Electrospray Droplets? When electrospray is used to generate the ions, the question arises whether the observed gas-phase ion intensity distributions are representative of the more stable nanoclusters ion clusters present in the supersaturated solution. A correlation might be present because, even though the solutions used are initially not saturated with the salt, there is extensive evaporation of the droplets before the gas-phase ions are generated, so that the solution in the droplets becomes saturated and supersaturated[12] by the time the ions are emitted into the gas phase. Even though the mechanism of ion production in the gas phase in not known in sufficient detail,[26] it is likely that the observed intensity distribution of clusters in the gas phase will reflect at least qualitatively the relative concentrations of different microcrystallites in the solution. To examine this possibility, NaCl solutions in water were sprayed with nanospray interfaced to a time-of-flight mass spectrometer that has a much higher mass range and resolution than the instrument used for the ion equilibrium determinations. For details, see the experimental part. The resulting mass spectra are shown in Figure 7. The two mass spectra were obtained with different drift field potentials of 50 and 450 V in the gas expansion zone. They represent only a sampling of results obtained with potentials at 25, 50, 160, 300, 350, and 450 V. At the lowest potential of 25 V, the total intensity was very low. This indicates that a potential above 25 V is required to drift the ions through the interface region. Therefore, the 50 V potential can be considered to lead to a condition where little or no excitation is imparted to the ions by the drift field. At the highest potential, 450 V, the magic number ions $Na(NaCl)_m^+$ with $m = 4$, 13, and 22 are clearly visible and dominate over neighboring peaks, while at the low potential of 50 V, the intensities appear to be much more evenly distributed. In particular, the magic ions with $m = 4$, 13, and 22 appear to have only slightly higher intensities than the neighboring peaks. Actually, the magic ions with $m = 13$ and 22 are much more prominent than it appears from Figure 7. This becomes clear from the expanded mass spectra shown in Figure 8. The spectrum at 50 V exhibits a number of doubly charged ions that are easily recognized by the presence of peaks that are one mass unit apart. When one subtracts the envelopes of these

(26) Gamaro-Castano M.; De la Mora, J. F. *J. Mass Spectrom.* **2000**, *35*, 790−803. (b) Kebarle, P.; Peschke, M. *Anal. Chim. Acta* **2000**, *406*, 11−35. (c) Kebarle, P. *J. Mass Spectrom.* **2000**, *35*, 804−817.

peaks, one finds that the remaining intensity, which is due to singly charged ions, leads to prominent $m = 13$ and $m = 22$ ions, but not a prominent $m = 4$ ion. This indicates that the $m = 13$ and 22 are magic ions also in the solution; i.e., they have concentrations higher that those of their neighbors. The mass range of the $m = 4$ ion (mass spectrum not shown) exhibited no prominent intensity of the $m = 4$ relative to the neighbor $m = 3$ and 5 ions. The same result is indicated from the mass spectrum obtained with the ion equilibrium instrument (see Figure 6).

The simplest spectrum is observed at 450 V (Figure 8B). Essentially only two singly charged ion groups are present: the $(NaCl)_{12}$ Na^+, which is small, and the $(NaCl)_{13}Na^+$, which is large. Because the doubly charged ions at 50 V were present at significant intensities and have disappeared, while the magic ions have grown at 450 V, the growth of the magic ions at 450 V must originate not only from the decomposition of singly charged higher mass ions but also, possibly predominantly, from the doubly charged ions. This result could have been expected because the doubly and multiply charged ions are less stable due to Coulomb repulsion.

Standing and co-workers[2c] concluded that the magic ions, when SIMS is used, originate from the decomposition of higher mass, singly charged, non-magic clusters $(MXM)_mM^+$ ions. For clusters produced by electrospray, the results shown in Figures 7 and 8 demonstrate that the magic ions originate not only from the decomposition of singly but also, to a very considerable extent, from doubly charged clusters. With electrospray, the magic distribution is very prominent when collisional decomposition is present. In the absence of collisional decomposition, the magic ions with $m = 13$ and 22 are still there but somewhat attenuated relative to the abundances observed at high excitation. On general grounds, magic (i.e., more stable) ions in the gas phase can be expected to be present at higher concentrations in supersaturated solutions. This expectation is supported by the present mass spectrometric results. The energy difference between stable and less stable ions in the gas phase may be reduced by solvation effects in solution. One can expect that the stable magic ions will be less stabilized by solvation than the non-magic ions, and therefore, their magic concentrations will be somewhat attenuated by this effect. The results presented in the preceding section that demonstrate weaker solvation on the magic ions in the gas phase provide support for this conclusion.

Acknowledgment. Financial support by the Natural Sciences and Engineering Research Council (NSERC), Canada, is acknowledged.

JA030663R